

Order–Disorder Transition in Supramolecular Polymers

Jessalyn Cortese, Corinne Soulié-Ziakovic, Michel Cloitre, Sylvie Tencé-Girault, and Ludwik Leibler*

Matière Molle et Chimie (UMR 7167 ESPCI-CNRS), ESPCI ParisTech, 10 rue Vauquelin 75005 Paris, France

S Supporting Information

ABSTRACT: In supramolecular polymers, directional interactions control the constituting units connectivity, but dispersion forces may conspire to make complex organizations. Here we report on the long-range order and order–disorder transition (ODT) of main-chain supramolecular polymers based on poly(propylene oxide) (PPO) spacers functionalized on both ends with thymine. Below the ODT temperature (T_{ODT}), these compounds are semicrystalline with a lamellar structure, showing nanophase separation between crystallized thymine planes and amorphous PPO layers. Above T_{ODT} , they are amorphous and homogeneous even though their X-ray scattering spectrum reveals a peak. This peak is due to correlation hole effect resulting from contrast between end-functional groups and spacer. Macroscopically, the transition is accompanied by dramatic flow and mechanical properties changes.

Block copolymers have attracted a great deal of interest in part because long-range ordered mesophases (such as lamellar, cylindrical, cubic or gyroid morphology) and order–disorder transition (ODT) can be achieved by simple control of the molecular parameters (degree of polymerization N and interaction parameter χ).¹ These two features are of great importance in technological applications ranging from cutting-edge electronic to bitumen additives.² The ability of a block copolymer to go from elastomeric-like (in its ordered state) to liquid-like (in its disordered state) properties by varying the temperature is particularly interesting.³ Since long-range ordered mesophases and ODT are also observed for liquid-crystals⁴ and supramolecular liquid crystals,⁵ the question of the existence and of the manifestations of long-range order and ODT in supramolecular polymers arises. Here we report on the long-range order lamellar structure and ODT of a main-chain supramolecular polymer.

Main-chain supramolecular polymers are typically made of telechelic molecules (A–spacer–A) linked together through non-covalent bonds to form a polymer-like assembly (A–spacer–A)_{*n*}.⁶ The self-complementary binding stickers (A) are often hydrogen bonding motifs such as nucleobases⁷ or ureidopyrimidinone,⁸ while the spacer is generally an oligomer.⁹ In these systems, microphase segregation between the spacer and the stickers,^{10–12} as well as crystallization of the stickers into microdomains^{13,14} can occur. Indeed, hydrogen bonding motifs are usually more polar than the spacer and are prone to crystallization. These two phenomena strongly impact the mechanical properties of the material: crystalline domains of stickers function as physical cross-links and induce elasticity-dominated rheological behavior;¹⁴

clusters of stickers can also result in a network that allows the formation of mechanically stable films.¹²

The microphase segregation phenomenon can manifest either as a nonordered clustering of the stickers¹¹ or as an ordered microphase separation as observed for block copolymers.¹ In fact, the telechelic molecule A–spacer–A can be seen as a triblock copolymer with the two outer blocks containing only one monomer. Cylindrical morphology has been reported for triblock copolymers with outer blocks containing nucleobase functionalities by Long¹⁵ or oligonucleotide by Matsushita.¹⁶ We anticipate that if incompatibility between the spacer and the sticker is strong, ordered mesophases should occur even for a single hydrogen-bonding group at both chain ends. Binder and his co-workers¹⁰ described the body-centered cubic (BCC) morphology of polyisobutylene monofunctionalized with diaminotriazine. The BCC structure was evidenced by regular peaks in the small-angle X-ray scattering pattern that disappeared above 90 °C. However, mesophases were not observed for the main-chain supramolecular polymer, polyisobutylene bifunctionalized with diaminotriazine.¹⁰

Different scenarios of disorder–order transition (DOT) from an homogeneous melt to an organized mesophase can be envisaged for main-chain supramolecular polymers (Figure 1). In the ordered state, various mesophases with segregated end-functional groups can be obtained. Depending on the system, the stickers atoms can present liquid-like correlations (Figure 1A,B) or long-range order, crystallization (Figure 1C). When the DOT is driven by the tendency of end-groups to crystallize, lamellar structure should be favored. In the disordered state, the scattering pattern is expected to display a low intensity peak (Figure 1D). The existence of such a peak does not imply local phase separation or clustering, but results from correlation hole effect.

The supramolecular polymers used in this study consist of low glass transition temperature (T_g), low molecular weight (460 and 2200 g·mol⁻¹), and noncrystalline poly(propylene oxide) (PPO) chains functionalized on both ends with thymine groups (Chart 1A). They are denoted as Thy–PPO- X –Thy, where X is the molecular weight (in g·mol⁻¹) of the PPO spacer. They were synthesized via amidation of diamine telechelic PPO with thymine-1-acetic acid (see Supporting Information). Thymine stickers can associate with one another through two hydrogen bonds (Chart 1B). Thymine dimerization is quite weak, as evidenced by its low thermodynamic association constant ($K_{\text{Thy–Thy}} = 4.3 \text{ M}^{-1}$, determined by ¹H NMR in CDCl₃).¹⁷ Another weak hydrogen bonding association can occur between two amide groups linking the thymine stickers to the PPO spacers, or between one amide group and one thymine motif. While the

Received: September 28, 2011

Published: November 10, 2011

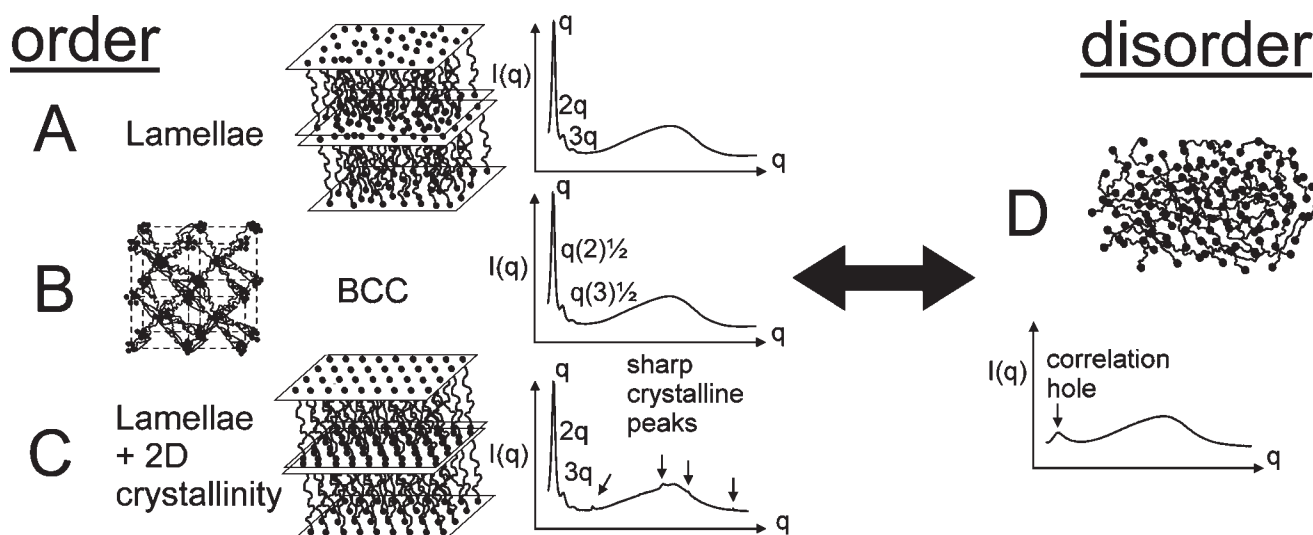
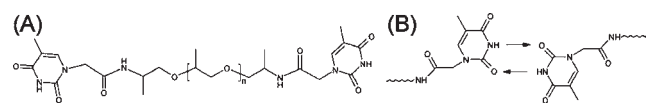


Figure 1. Possible scenarios for order–disorder transition in main-chain telechelic self-complementary supramolecular polymers and associated X-ray spectra. Ordered mesophase in a lamellar (A) or BCC (B) morphology with liquid-like correlations of the stickers atoms inside the structure. Ordered mesophase in a lamellar morphology with crystallinity of the stickers atoms inside the lamellar planes (C). Disordered state (D).

Chart 1. (A) Thy–PPO–X–Thy and (B) Thy Self-Association



PPO chain is hydrophobic, thymine is polar. Besides, thymine derivatives readily crystallize. Therefore, three different phenomena concur and compete in the bulk: hydrogen bonding, microphase segregation between the PPO chains and the thymine stickers, and crystallization of thymines into microdomains. The bulk structure and properties of the Thy–PPO–X–Thy ($X = 460, 2200$) compounds were investigated by structural (polarized optical microscopy, X-ray scattering), thermal (differential scanning calorimetry (DSC)) and rheological characterizations. X-ray scattering were performed at the SOLEIL Synchrotron source in France with the beamline SWING enabling simultaneous small-angle and wide-angle X-ray scattering measurements.

Thy–PPO–X–Thy ($X = 460, 2200$) display on DSC (Supporting Information) a glass transition step, an exotherm reminiscent of crystallization, and an endotherm reminiscent of melting. After a heating cycle, Thy–PPO–2200–Thy crystallizes during the cooling cycle at $10\text{ }^{\circ}\text{C}/\text{min}$, while Thy–PPO–460–Thy only crystallizes during the next heating cycle (cold crystallization), revealing that Thy–PPO–460–Thy crystallization is a slower process than that of Thy–PPO–2200–Thy. Indeed, the T_g of Thy–PPO–460–Thy is much higher than that of Thy–PPO–2200–Thy. So, at the same temperature Thy–PPO–2200–Thy has a higher mobility than Thy–PPO–460–Thy. If the materials are given time to anneal at temperatures below the melting temperature ($T_m = 67\text{ }^{\circ}\text{C}$ for Thy–PPO–2200–Thy and $T_m = 109\text{ }^{\circ}\text{C}$ for Thy–PPO–460–Thy) but above the crystallization temperature, the extent of crystallization increases, as reflected by the enthalpy of fusion (ΔH_f) increase. In fact, ΔH_f increases dramatically for Thy–PPO–460–Thy (from 9 to 33 J/g), but only slightly for Thy–PPO–2200–Thy (from 15 to 18 J/g) upon

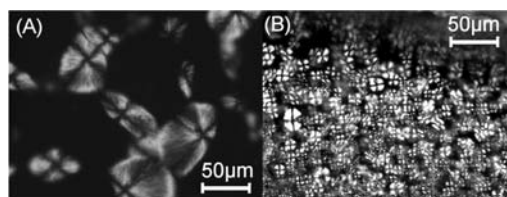


Figure 2. Polarized optical microscopy of (A) Thy–PPO–460–Thy and (B) Thy–PPO–2200–Thy.

annealing. Polarized optical microscopy images of these materials (Figure 2) show bright spherulite-like spots with a Maltese cross extinction along the polarization axes of the crossed polarizer and analyzer, characteristic of anisotropy.

X-ray diffraction (XRD) spectra at $30\text{ }^{\circ}\text{C}$ of Thy–PPO–2200–Thy (Figure 3A and 3C) and Thy–PPO–460–Thy (Supporting Information) show a broad band between $q = 0.6\text{ }^{\circ}\text{Å}^{-1}$ (corresponding to $d = 10.5\text{ }^{\circ}\text{Å}$) and $q = 2.4\text{ }^{\circ}\text{Å}^{-1}$ ($d = 2.6\text{ }^{\circ}\text{Å}$) characteristic of nearest neighbors correlation in amorphous phases. This broad halo contains sharp peaks characteristic of crystallinity. These results indicate that Thy–PPO–X–Thy ($X = 460, 2200$) are semi-crystalline. The sharp peaks corresponding to d spacing of 4.0, 4.8, and 11.9 $^{\circ}\text{Å}$ are common to Thy–PPO–460–Thy and Thy–PPO–2200–Thy. We attribute these peaks to the crystallization of thymine end groups in microdomains.¹⁸ Thus, the crystallinity concerns only the thymine moieties, while the rest of the PPO chain remains amorphous. This picture is consistent with the fact that diamine telechelic PPO is amorphous and thymine is crystalline, and with the fact that the value of the enthalpy of fusion ΔH_f of annealed Thy–PPO–460–Thy is much greater than that of annealed Thy–PPO–2200–Thy (33 J/g compared to 18 J/g). Indeed, the percentage of thymine moieties is much higher in Thy–PPO–460–Thy than in Thy–PPO–2200–Thy.

In addition to the crystalline order, long-range ordering is also found for Thy–PPO–X–Thy ($X = 460, 2200$). Thy–PPO–2200–Thy reveals peaks corresponding to 60 $^{\circ}\text{Å}$ (q), 30 $^{\circ}\text{Å}$ ($2q$), 20 $^{\circ}\text{Å}$ ($3q$) and 15 $^{\circ}\text{Å}$ ($4q$), that are consistent with a lamellar order

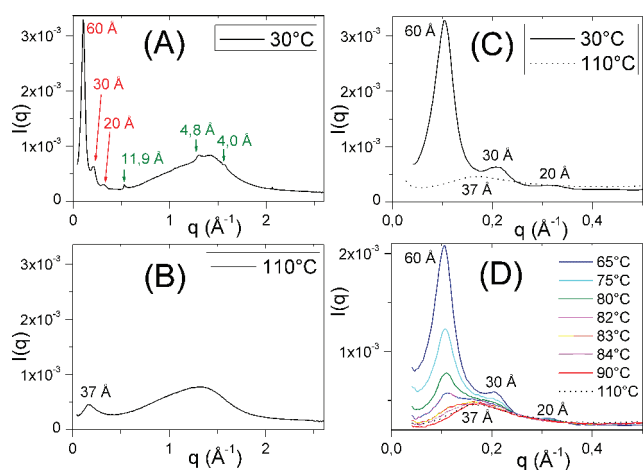


Figure 3. XRD of Thy–PPO-2200–Thy at 30 °C (A) and 110 °C (B); enlargement of the small q range at 30 and 110 °C (C) and around the ODT ($T_{\text{ODT}} = 85$ °C) (D).

of spacing $d = 60$ Å. Annealed Thy–PPO-460–Thy (Supporting Information) displays peaks corresponding to 27.7 Å (q) and 13.3 Å ($2q$) clearly defined, as well as 8.6 Å ($3q$), 6.7 Å ($4q$), 5.3 Å ($5q$), and 3.4 Å ($8q$) less defined. The regular spacing is consistent with a lamellar order of spacing $d = 27.7$ Å. Without annealing, the peaks corresponding to the lamellar order are shifted to shorter distances, whereas the peaks corresponding to the crystalline order remain at the same position. The lamellar d spacing of Thy–PPO-460–Thy increases from 20.6 to 27.7 Å after annealing at 100 °C.

To conclude, under T_m Thy–PPO- X –Thy ($X = 460, 2200$) are semicrystalline and exhibit two distinct orders: a crystalline order and a lamellar order. The lamellar structure is constituted of alternating two-dimensional (2D) crystallized thymine planes and amorphous PPO layers (Figure 1.C). Additional hydrogen bonding between the amide groups linking the thymine to the PPO chain may further stabilize this organization. The annealing allows the PPO chains to stretch more and thus increases the lamellar spacing. Yet, the chains remain partially folded and stay amorphous. Temperature-dependent XRD measurements of Thy–PPO- X –Thy ($X = 460, 2200$) (Supporting Information) show that the two orders, crystalline and lamellar, disappear together on heating around the DSC melting temperature T_m . The transition is reversible upon cooling. So, the DSC melting endotherm and crystallization exotherm can be attributed to the simultaneous (on the time scale of our temperature dependent XRD experiments) destruction and formation, respectively, of these two orders. So, it seems that, in analogy with block copolymers consisting of amorphous and crystallizable blocks, the crystallization is confined in the lamellar planes not because the melt morphology was retained during crystallization but because of crystallization-driven microphase segregation.¹⁹

At higher temperature, above T_m , in addition to the nearest neighbors correlation halo, a peak that scales with the chain length is observed on the XRD spectra of Thy–PPO-2200–Thy (Figure 3B and 3C) and Thy–PPO-460–Thy (Supporting Information). This peak is clearly not a sign of a long-range correlated nanostructure, since there are no higher order reflections. However, it could still be argued that it reflects a short-range fluctuating nanoscale segregation. Yet, we interpret this peak as resulting from the correlation hole effect:^{1a,20} it reflects

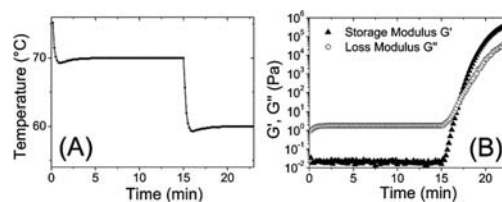


Figure 4. Rheology of Thy–PPO-2200–Thy during a temperature jump: (A) temperature jump from 70 to 60 °C and (B) transition from viscous flow to elastic behavior after the temperature jump from 70 to 60 °C.

the typical distance between strong scattering polar stickers separated by the PPO chain, hence the chain length scaling, but it does not indicate mesoscopic segregation. Indeed, this peak's intensity is very low compared to the nearest neighbors correlation halo and its width is very broad compared to the lamellar order Bragg peak. It should be stressed here that the visibility of the correlation hole peak depends on the contrast between the spacer and the stickers, and that while with our system this peak is clearly visible with a synchrotron radiation, it was barely noticeable with a sealed tube X-ray generator radiation. Plus, comparison with a simple model^{1a} of the correlation hole peaks in corresponding block copolymers seems to further support this interpretation (Supporting Information).

Consequently, Thy–PPO- X –Thy ($X = 460, 2200$) are in a disordered state above T_m . The transition at T_m is then an ODT that takes place in just a few degrees as evidenced by the dramatic evolution of the XRD spectra in the small q range during an heating ramp at 10 °C per minute (Figure 3D). The slight shift in temperature compared to the DSC T_m is related to the setup and thermoinertia resulting from the ramp.

This image of ODT is nicely confirmed by the rheological study and supports an analogy with crystallizable block copolymers.²¹ Indeed, the frequency sweep of Thy–PPO-2200–Thy above 70 °C, in the molten disordered state, is characteristic of a viscous fluid in the terminal flow regime (Supporting Information). However, a transition from viscous flow to elastic behavior is observed in a few minutes after a temperature jump from 70 to 60 °C (Figure 4). At 60 °C, under $T_{\text{ODT}} = 67$ °C, the storage modulus G' becomes higher than the loss modulus G'' . The transition is reversible upon heating. These results suggest that crystalline planes of thymine act as physical cross-links, causing rheological behavior typical of a viscoelastic solid.

In summary, we have demonstrated the existence of a long-range order and of an order–disorder transition in a telechelic supramolecular system. Under T_{ODT} , a lamellar structure with alternating amorphous chains and 2D crystallized stickers plane is formed. This organization is favorable as it allows microphase segregation of the hydrophobic spacer and polar sticker, as well as dimerization of the stickers by hydrogen bonding and 2D-crystallization of the stickers. Because of this structuration, the material behaves like a semicrystalline polymer: liquid over T_{ODT} and viscoelastic solid below. Besides, we have underlined the importance of taking into account the correlation hole effect to interpret X-ray scattering spectra of the disordered state, to avoid confusion between a cluster peak and an homogeneous state correlation hole peak. Finally, whether the long-range order and ODT can be observed in a main-chain supramolecular polymer with no crystallization remains an open question. Development of models taking into account dispersion forces as well as

directional associations²² should pave the way to better control of supramolecular polymers organization and properties.

■ ASSOCIATED CONTENT

S Supporting Information. Synthesis procedure and characterization (¹H and ¹³C NMR, DSC, X-ray scattering, rheology) of Thy–PPO–X–Thy (X = 460, 2200); correlation hole modelization. This material is available free of charge via the Internet at <http://pubs.acs.org>.

■ AUTHOR INFORMATION

Corresponding Author

ludwik.leibler@espci.fr

■ ACKNOWLEDGMENT

We thank SOLEIL for provision of synchrotron radiation facilities and Florian Meneau for assistance in using beamline SWING. We are grateful to Huntsman for providing Jeffamine D. We are indebted to Alexandre Prevot for preparation and characterization of Thy–PPO-460–Thy. We thank Damien Montarnal and François Tournilhac for discussions.

■ REFERENCES

- (1) (a) Leibler, L. *Macromolecules* **1980**, *13*, 1602. (b) Fredrickson, G. H.; Helfand, E. *J. Chem. Phys.* **1987**, *87*, 697. (c) Bates, F. S.; Rosedale, J. H.; Fredrickson, G. H. *J. Chem. Phys.* **1990**, *92*, 6255.
- (2) (a) Lodge, T. P. *Macromol. Chem. Phys.* **2003**, *204*, 265. (b) Park, C.; Yoon, J.; Thomas, E. L. *Polymer* **2003**, *44*, 6725.
- (3) Bates, F. S.; Fredrickson, G. H. *Annu. Rev. Phys. Chem.* **1990**, *41*, 525.
- (4) De Gennes, P. G.; Prost, J. *The Physics of Liquid Crystals*; Oxford University Press: Oxford, 1993.
- (5) (a) Kato, T.; Frechet, J. M. J. *J. Am. Chem. Soc.* **1989**, *111*, 8533. (b) Kato, T.; Frechet, J. M. J. *Liq. Cryst.* **2006**, *33*, 1429.
- (6) (a) Lehn, J.-M. *Prog. Polym. Sci.* **2005**, *30*, 814. (b) Fox, J. D.; Rowan, S. J. *Macromolecules* **2009**, *42*, 6823. (c) de Greef, T. F. A.; Smulders, M. M. J.; Wolfs, M.; Schenning, A. P. H. J.; Sijbesma, R. P.; Meijer, E. W. *Chem. Rev.* **2009**, *109*, 5687. (d) Serpe, M. J.; Craig, S. L. *Langmuir* **2007**, *23*, 1626.
- (7) Sivakova, S.; Rowan, S. J. *Chem. Soc. Rev.* **2005**, *34*, 9.
- (8) Sijbesma, R. P.; Beijer, F. H.; Brunsveld, L.; Folmer, B. J. B.; Hirschberg, J. H. K. K.; Lange, R. F. M.; Lowe, J. K. L.; Meijer, E. W. *Science* **1997**, *278*, 1601.
- (9) (a) Binder, W. H.; Zirbs, R. *Adv. Polym. Sci.* **2007**, *207*, 1. (b) Bouteiller, L. *Adv. Polym. Sci.* **2007**, *207*, 79.
- (10) Herbst, F.; Schröter, K.; Gunkel, I.; Gröger, S.; Thurn-Albrecht, T.; Balbach, J.; Binder, W. H. *Macromolecules* **2010**, *43* (23), 10006.
- (11) (a) de Lucca Freltas, L.; Burgert, J.; Stadler, R. *Polym. Bull.* **1987**, *17*, 431. (b) Folmer, B. J. B.; Sijbesma, R. P.; Versteegen, R. M.; van der Rijt, J. A. J.; Meijer, E. W. *Adv. Mater.* **2000**, *12*, 874. (c) Yamauchi, K.; Lizotte, J. R.; Hercules, D. M.; Vergne, M. J.; Long, T. E. *J. Am. Chem. Soc.* **2002**, *124*, 8599. (d) Öjelund, K.; Loontjens, T.; Steeman, P.; Palmans, A.; Maurer, F. *Macromol. Chem. Phys.* **2003**, *204*, 52. (e) Mather, B. D.; Elkins, C. L.; Beyer, F. L.; Long, T. E. *Macromol. Rapid Commun.* **2007**, *28*, 1601. (f) Botterhuis, N. E.; van Beek, D. J. M.; van Gemert, G. M. L.; Bosman, A. W.; Sijbesma, R. P. *J. Polym. Sci., Part A: Polym. Chem.* **2008**, *46*, 3877. (g) Merino, D. H.; Slark, A. T.; Colquhoun, H. M.; Hayes, W.; Hamley, I. W. *Polym. Chem.* **2010**, *1*, 1263. (h) Woodward, P. J.; Hermida Merino, D.; Greenland, B. W.; Hamley, I. W.; Light, Z.; Slark, A. T.; Hayes, W. *Macromolecules*

2010, *43*, 2512. (i) Manassero, C.; Raos, G.; Allegra, G. *J. Macromol. Sci. B* **2005**, *44*, 855. (j) Podesva, J.; Dybal, J.; Spevacek, J.; Stepanek, P.; Cernoch, P. *Macromolecules* **2001**, *34*, 9023.

(12) (a) Sivakova, S.; Bohnsack, D. A.; Mackay, M. E.; Suwanmala, P.; Rowan, S. J. *J. Am. Chem. Soc.* **2005**, *127*, 18202. (b) Beck, J. B.; Ineman, J. M.; Rowan, S. J. *Macromolecules* **2005**, *38*, 5060.

(13) (a) Hilger, C.; Stadler, R. *Macromolecules* **1992**, *25*, 6670. (b) Hirschberg, J. H. K. K.; Beijer, F. H.; van Aert, H. A.; Magusin, P. C. M. M.; Sijbesma, R. P.; Meijer, E. W. *Macromolecules* **1999**, *32*, 2696. (c) van Beek, D. J. M.; Spiering, A. J. H.; Peters, G. W. M.; te Nijenhuis, K.; Sijbesma, R. P. *Macromolecules* **2007**, *40*, 8464.

(14) (a) Lillya, C. P.; Baker, R. J.; Hutte, S.; Winter, H. H.; Lin, Y. G.; Shi, J.; Dickinson, L. C.; Chien, J. C. W. *Macromolecules* **1992**, *25*, 2076. (b) Muller, M.; Dardin, A.; Seidel, U.; Balsamo, V.; Ivan, B.; Spiess, H. W.; Stadler, R. *Macromolecules* **1996**, *29*, 2577. (c) Colombani, O.; Barioz, C.; Bouteiller, L.; Chanéac, C.; Fompérie, L.; Lortie, F.; Montès, H. *Macromolecules* **2005**, *38*, 1752. (d) Dankers, P. Y. W.; Zhang, Z.; Wisse, E.; Grijpma, D. W.; Sijbesma, R. P.; Feijen, J.; Meijer, E. W. *Macromolecules* **2006**, *39*, 8763. (e) van Beek, D. J. M.; Gillissen, M. A. J.; van As, B. A. C.; Palmans, A. R. A.; Sijbesma, R. P. *Macromolecules* **2007**, *40*, 6340. (f) Wietor, J.-L.; van Beek, D. J. M.; Peters, G. W.; Mendes, E.; Sijbesma, R. P. *Macromolecules* **2011**, *44*, 1211.

(15) Mather, B. D.; Baker, M. B.; Beyer, F. L.; Berg, M. A. G.; Green, M. D.; Long, T. E. *Macromolecules* **2007**, *40*, 6834.

(16) Noro, A.; Nagata, Y.; Tsukamoto, M.; Hayakawa, Y.; Takano, A.; Matsushita, Y. *Biomacromolecules* **2005**, *6*, 2328.

(17) Beijer, F. H.; Sijbesma, R. P.; Vekemans, J. A. J. M.; Meijer, E. W.; Kooijman, H.; Spek, A. L. *J. Org. Chem.* **1996**, *61*, 6371.

(18) Shimizu, T.; Iwaura, R.; Masuda, M.; Hanada, T.; Yase, K. *J. Am. Chem. Soc.* **2001**, *123*, 5947.

(19) (a) Xu, J.-T.; Turner, S. C.; Fairclough, J. P. A.; Mai, S.-M.; Ryan, A. J.; Chaibundit, C.; Booth, C. *Macromolecules* **2002**, *35*, 3614. (b) Rangarajan, P.; Register, R. A.; Adamson, D. H.; Fetters, L. J.; Bras, W.; Naylor, S.; Ryan, A. J. *Macromolecules* **1995**, *28*, 1422.

(20) Bates, F. S. *Macromolecules* **1985**, *18*, 525.

(21) (a) Hamley, I. *Adv. Polym. Sci.* **1999**, *148*, 113. (b) Deplace, F.; et al. *J. Polym. Sci. B: Polym. Phys.* **2010**, *48*, 1428.

(22) Hoy, R. S.; Fredrickson, G. H. *J. Chem. Phys.* **2009**, *131*, 224902.